J. Fluid Mech. (1969), *vol.* 36, *part* 3, *pp.* 465–480
Printed in Great Britain

Instability and river channels

By R. A. CALLANDER
School of Engineering, University of Auckland, New Zealand

(Received 9 November 1967 and in revised form 12 November 1968)

A linearized stability analysis of the flow of water in a channel with a loose bed and straight banks is described. It is assumed that the wavelength of the perturbations, which develop into meanders or braids, is longer than the width of the channel. It is therefore long compared with the ripples or dunes which cover the bed of such a channel and whose wavelength is shorter than the width of the channel. The latter need be allowed for only as roughness elements creating resistance. The variation of resistance to flow and rate of transport of bed material with velocity are discussed briefly and taken into account. Instability is interpreted as leading to a meandering or braided channel and it is shown that all practicable channels are unstable. Wavelengths calculated for channels expected to meander are compatible with those given by Inglis's empirical rule and wavelengths calculated for channels which become braided are approximately the same as those observed.

1. Introduction

Meandering and braided channels have two characteristics of interest. The first is that they occur at all and the second is the strength of empirical relationships between meander dimensions and rate of flow. In this paper, it is assumed that meanders and braids occur because of instability and a linearized analysis is used to classify individual channels as stable or unstable and to calculate the wavelength of the meandering or braided pattern which will develop.

The concept of dynamic instability and reasoning based on it have appeared in several papers about channels with loose boundaries. White (1939, 1948) suggested, as a result of his experiments, that instability of the bed is the cause of meandering. Kennedy (1963), Reynolds (1965) and Hansen (1967) presented theoretical studies of the stability of erodible channels. Kennedy and Reynolds investigated the occurrence of ripples, dunes and antidunes on the bed and Reynolds, in addition, discussed meanders. Hansen's paper is about meanders.

2. Qualitative analysis

The mechanism whereby a disturbance to the flow in an erodible channel may cause an increase in its own amplitude can be discussed qualitatively. Figure 1 (*a*) is a plan view of a straight channel showing five streamlines, all initially straight. These have been deformed by an arbitrary periodic disturbance. Assuming that the Bernoulli equation can be used for this qualitative discussion only, consideration of energy and continuity shows that the surface is lowered on the inside of a curve (at A and C, for example) and the velocity increased. On the outside of a curve (e.g. at B) the surface is raised and the velocity reduced (figure 1 (b)). That is to say, the velocity of the water decreases as it flows from A to B and increases as it flows from B to C. Assuming that the rate of transport of bed load increases with velocity, the bed must rise between A and B and fall between B and C as time passes. This will happen if a wave forms on the bed as shown in figure 1 (c),

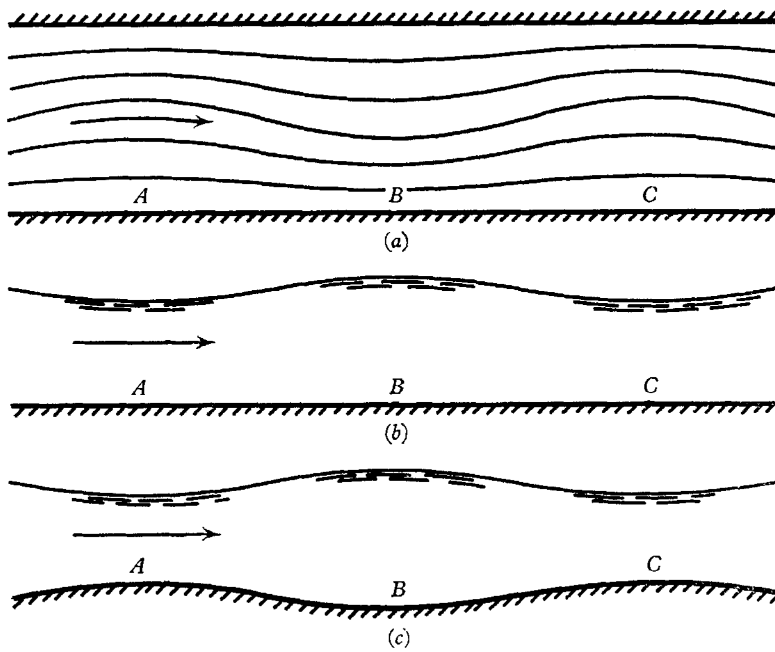

FIGURE 1. Sketches of disturbed flow. (a) Plan. (b), (c) Elevations.

the wave travelling downstream. If the flow is subscritical (Froude number less than 1) these changes of bed level will cause a further lowering of the surface at A and C and an increase in surface elevation at B. Thus, the initial changes bring about further changes of the same sign. The time scale of these changes is large.

This tendency towards instability may be modified by the characteristics of the resistance to flow. Vanoni & Brooks (1957), Raudkivi (1963) and Kennedy & Brooks (1965) have shown how the drag coefficient f for an erodible bed varies with velocity. Consequently, the bed shear stress $\tau \; (= \frac{1}{8} f \rho V^2)$ is also a function of velocity V and figure 4 shows typical curves. (The data on which these are based are discussed later.) If the bed material is fine grained, there may be a range of velocity through which the bed shear stress decreases as the velocity increases. Then, an increase in velocity can, by making the bed less rough, cause a further increase.

The characteristics of the resistance curve are such as to increase the instability inherent in the relationship for rate of transport of bed load when the bed shear stress decreases with increase of velocity and to decrease it when the bed shear stress increases with velocity. It must be emphasized that the stabilizing effect of the positive slope of the bed shear stress curve may not be great enough to reverse the tendency towards instability caused by positive slope of the bed load transport curve.

This argument is not precise or complete, but it does show a mechanism of instability. The following mathematical argument leads to conclusions which are more precise, within the limitations of the assumptions.

3. Equations of motion

The linearized stability analysis is used to investigate the flow in a wide shallow channel and the undisturbed flow is taken to be steady and uniform. Because the bed is deformed into the appropriate configuration of small moving bed features, the flow is not, in fact, either steady or uniform. However, it is assumed that these bed features can be taken as the cause, along with surface drag, of the resistance to flow, but can be otherwise ignored.

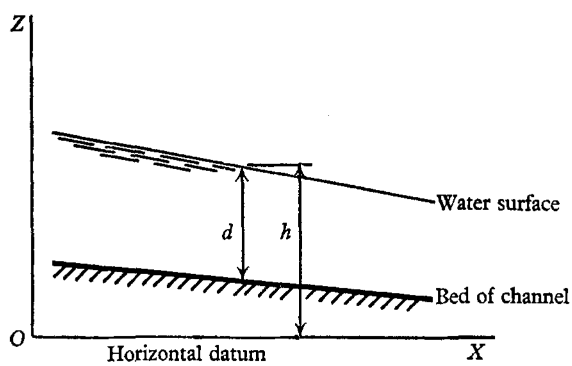

FIGURE 2. Vertical section on centre line of channel illustrating system of co-ordinates, OX, OY (not shown) and OZ are a right-handed Cartesian set of axes.

The co-ordinate system is defined in figure 2, the axis OX being horizontal and in the same vertical plane as the centre line of the channel. OY is horizontal and transverse to the channel centre line and OZ is vertical. The depth of flow at any point is d and the elevation of the surface above a horizontal datum is h. The mean slope of the ripple or dune covered bed is S_0, positive when the bed descends in the direction of flow. Since S_0 is small, the velocity along the channel parallel to the bed is assumed to be equal to u, the component parallel to OX.

The force–momentum equations for unit volume of water are

$$\rho\frac{\partial u}{\partial t}+\rho u\frac{\partial u}{\partial x}+\rho v\frac{\partial u}{\partial y} = -\gamma\frac{\partial h}{\partial x}-\frac{\tau}{d}, \tag{1}$$

$$\rho\frac{\partial v}{\partial t}+\rho u\frac{\partial v}{\partial x}+\rho v\frac{\partial v}{\partial y} = -\gamma\frac{\partial h}{\partial y}-\frac{v}{V}\frac{\tau}{d}. \tag{2}$$

The equation of continuity for the water is

$$\frac{\partial}{\partial x}(ud)+\frac{\partial}{\partial y}(vd)+\frac{\partial d}{\partial t}=0 \tag{3}$$

and the equation of continuity for the bed material is

$$\frac{\partial}{\partial t}(h-d)+\frac{\partial L}{\partial x}+\frac{\partial}{\partial y}\left(\frac{v}{V}L\right)=0. \tag{4}$$

These three terms represent the rate at which bed material is stored in an elementary stationary control volume, the net rate of outflow from the control volume in the direction of increasing x and the net rate of outflow in the direction of increasing y.

The density of the fluid is ρ, γ is its specific weight, τ is the bed shear stress and L is the rate of transport of bed load in units of space occupied in the bed per unit of time per unit of width of the channel.

The following assumptions have been made: (*a*) the velocity is uniformly distributed through the depth of flow and the vertical component is zero; (*b*) the pressure distribution is hydrostatic; (*c*) the gradient of shear stress, τ_{zx}, through the depth of flow is constant and equal to its average τ/d (τ_{zx} is the component of shear stress parallel to OX on a surface normal to OZ); (*d*) the gradient of shear stress, τ_{yx}, across the flow is zero (τ_{yx} is the component of shear stress parallel to OX on a surface normal to OY); (*e*) the bed shear stress is parallel to the resultant velocity V, which is the vector sum of the components u and v; (*f*) the movement of the bed load is in the direction of the resultant velocity.

Assumptions (*a*) and (*e*) imply that secondary currents have been ignored. These currents are driven by superelevation of the surface and, even in a bend with pronounced curvature, they are small relative to the lontigudinal velocity. In this analysis infinitesimal disturbances to flow in a straight channel are investigated so that superelevation of the surface is infinitesimal; it is assumed that the secondary currents driven by this small transverse slope are an order of size smaller than the perturbations to the components of velocity.

These equations must be satisfied for the initial undisturbed flow when $u = U$, $v = 0$, $d = d_0$, $\tau = \tau_0$, $L = L_0$ and $h = h_0 - S_0 x$, whence

$$\tau_0 = \gamma d_0 S_0. \tag{5}$$

They must also be satisfied for the perturbed motion when $u = U+u'$, $v = v'$, $d = d_0+d'$, $\tau = \tau_0+\tau'$, $L = L_0+L'$ and $h = h_0-S_0x+h'$. Substitution of these and (5) in (1)–(4) yields, after dropping products and powers of the primed variables and their differentials as second-order small quantities

$$\rho\frac{\partial u'}{\partial t}+\rho U\frac{\partial u'}{\partial x}=-\gamma\frac{\partial h'}{\partial x}-\frac{\tau'}{d_0}+\gamma S_0\frac{d'}{d_0}, \tag{6}$$

$$\rho\frac{\partial v'}{\partial t}+\rho U\frac{\partial v'}{\partial x}=-\gamma\frac{\partial h'}{\partial y}-\frac{v'}{U}\frac{\tau_0}{d_0}, \tag{7}$$

$$d_0\frac{\partial u'}{\partial x}+U\frac{\partial d'}{\partial x}+d_0\frac{\partial v'}{\partial y}+\frac{\partial d'}{\partial t}=0, \tag{8}$$

$$\frac{\partial h'}{\partial t}-\frac{\partial d'}{\partial t}+\frac{\partial L'}{\partial x}+\frac{L_0}{U}\frac{\partial v'}{\partial y}=0. \tag{9}$$

4. Resistance to flow and rate of transport of bed load

Equations (6)–(9) contain six variables, the disturbances to the components of velocity, depth, surface elevation, bed shear stress and rate of transport of bed load. To proceed further, two more equations are required. It is assumed that bed shear stress and rate of transport of bed load are both functions of velocity. Both dependent variables are averaged over an area of the order of size of one bed feature, i.e. one ripple or dune. (These ripples or dunes are created by the flow and are of appreciably smaller wavelength than the disturbance to the mean bed profile.) In this way the effects of surface drag and form drag are both included. The local average drag and transport rate vary over the wavelength of the main disturbance and the width of the channel.

It is not possible to quote equations which are generally applicable and the necessary functions must be found by experiment. The shape of the curve relating bed shear stress to mean velocity is well established from the experiments of Vanoni & Brooks (1957), Raudkivi (1963, 1967) and Kennedy & Brooks (1965). It consists of a base parabola corresponding to surface drag on a flat bed and, superimposed on the parabola, the form drag which first increases with velocity, then decreases as the bed features are erased.

Formulas for rate of transport of bed load usually have a bed shear stress for their argument. However, it is not clear how much the form drag contributes to transport of bed load, because it does not do so directly. The form drag on one of the small scale bed features is related to the fluid shear in the shear layer between the separated flow and the wake in the lee of the bed feature. Turbulence generated in the shear layer agitates the grains of the bed, where it reattaches and for some distance downstream, so increasing the mobility of the grains. Not all of the form drag is effective in this way because not all of the turbulence generated in the shear layer survives near the bed. Experiments show that bed load transport can be correlated with mean velocity so that the parts played by surface drag and form drag need not be known for this analysis.

Experimentally determined functions relating bed shear stress and rate of transport of bed load are assumed to be available for any particular channel. Then, τ' and L' can be eliminated by using

$$\tau' = m_1 u', \tag{10}$$

$$L' = m_2 u', \tag{11}$$

where m_1, m_2 are the local slopes of the respective functions.

5. Stability analysis

Using (10), (11), the equations of motion become, after rearrangement

$$\frac{1}{g}\frac{\partial u'}{\partial t} + \frac{U}{g}\frac{\partial u'}{\partial x} = -\frac{\partial h'}{\partial x} - S_0\left(\frac{m_1 u'}{\tau_0} - \frac{d'}{d_0}\right), \tag{12}$$

$$\frac{1}{g}\frac{\partial v'}{\partial t} + \frac{U}{g}\frac{\partial v'}{\partial x} = -\frac{\partial h'}{\partial y}S_0 - \frac{v'}{U}, \tag{13}$$

$$d_0\frac{\partial u'}{\partial x}+U\frac{\partial d'}{\partial x}+d_0\frac{\partial v'}{\partial y}+\frac{\partial d'}{\partial t}=0, \tag{14}$$

$$\frac{\partial h'}{\partial t}-\frac{\partial d'}{\partial t}+m_2\frac{\partial u'}{\partial x}+\frac{L_0}{U}\frac{\partial v'}{\partial y}=0. \tag{15}$$

The solution postulated is

$$u' = AU\exp\left\{ikS_0\left(\frac{x-cUt}{d_0}\right)\right\},$$

$$v' = BU\exp\left\{ikS_0\left(\frac{x-cUt}{d_0}\right)\right\},$$

$$d' = Dd_0\exp\left\{ikS_0\left(\frac{x-cUt}{d_0}\right)\right\},$$

$$h' = Hd_0\exp\left\{ikS_0\left(\frac{x-cUt}{d_0}\right)\right\}.$$

A, B, D and H are dimensionless complex functions of y, k is the dimensionless wave-number of each sinusoidal disturbance and $c = c_r+ic_i$ is the dimensionless complex celerity. Equations (10), (11) imply that τ' and L' are in phase with u'. The other disturbances v', d' and h' will, in general, not be in phase with u', the phase displacement being given by the real and imaginary parts of A, B, D and H.

Substitution of the postulated solution in (12)–(15) leads to the following set:

$$\{m_1U/\tau_0+ikF_0^2(1-c)\}A-D+ikH=0, \tag{16}$$

$$\{1+ikF_0^2(1-c)\}B=-(d_0/S_0)H', \tag{17}$$

$$A+(1-c)D=i\frac{1}{k}\frac{d_0}{S_0}B', \tag{18}$$

$$\frac{m_2}{d_0}A+cD-cH=i\frac{L_0}{Ud_0}\frac{1}{k}\frac{d_0}{S_0}B'. \tag{19}$$

B' and H' are the differentials with respect to y of B and H respectively and $F_0 = U/\sqrt{(g\,d_0)}$ is the Froude number of the undisturbed flow.

When A and D are eliminated from (16), (18) and (19) the result gives H in terms of B'. This equation can then be used with (17) to eliminate H and the resulting ordinary differential equation is

$$B''+\lambda B=0, \tag{20}$$

where λ is a complex eigenvalue given by

$$\lambda=\frac{kS_0^2}{d_0^2}\frac{\{kF_0^2(1-c)-i\}(\det C)}{\left(\frac{L_0}{Ud_0}-\frac{m_2}{d_0}\right)+\left\{\frac{m_1U}{\tau_0}+ikF_0^2(1-c)\right\}\left\{\frac{L_0}{Ud_0}(1-c)-c\right\}}, \tag{21}$$

$$\det C=\begin{vmatrix}\{m_1U/\tau_0+ikF_0^2(1-c)\} & -1 & ik\\ 1 & 1-c & 0\\ m_2/d_0 & c & -c\end{vmatrix}.$$

The boundary condition to be satisfied by (20) is $B = 0$ at $y = \pm b$, where b is the half width of the channel. This requirement has to be satisfied for the banks to remain straight and parallel. (Growth of an unstable perturbation to the bed will lead to a single or multiple thread pattern of alternating pools and bars. If the banks cannot resist erosion a meander will develop from the initial disturbance to the bed of the straight channel.)

To satisfy the boundary condition it is necessary that

$$\operatorname{Re}\lambda > 0,$$
$$\operatorname{Im}\lambda = 0,$$

and the solution for B is

$$B = P\cos n\frac{\pi}{2}\frac{y}{b} \quad (n = 1, 3, 5, \ldots). \tag{22}$$

Hence

$$\lambda = (n\pi/2b)^2$$

and

$$\frac{d_0^2}{kS_0^2}\lambda = \frac{\nu^2}{k}, \tag{23}$$

where

$$\nu = \frac{n\pi}{S_0}\frac{d_0}{2b}.$$

Using (23) in (21)

$$\frac{\nu^2}{k} = \frac{\{kF_0^2(1-c)-i\}(\det C)}{\left(\dfrac{L_0}{Ud_0}-\dfrac{m_2}{d_0}\right)+\left\{\dfrac{m_1U}{\tau_0}+ikF_0^2(1-c)\right\}\left\{\dfrac{L_0}{Ud_0}(1-c)-c\right\}}. \tag{24}$$

Equation (24) is reduced to a pair of linear simultaneous equations in c_r and c_i by expanding the right side and making use of the fact that certain variables are small, as follows:

$$kF_0^2 \ll 1,$$
$$c_r \ll 1,$$
$$m_2/d_0 \ll 1,$$
$$L_0/Ud_0 \ll 1,$$
$$L_0/Ud_0 - c_r \ll 1.$$

Products and powers of c_r, c_i are also negligible. The linear equations obtained are

$$a_{11}c_r + a_{12}c_i = b_1, \tag{25}$$
$$a_{21}c_r + a_{22}c_i = b_2, \tag{26}$$

where

$$a_{11} = -kF_0^2\left(1+\frac{m_1U}{\tau_0}\right)+k(1-F_0^2)+\frac{\nu^2}{k}\frac{m_1U}{\tau_0},$$

$$a_{12} = -k^2F_0^2(1-F_0^2)-\left(1+\frac{m_1U}{\tau_0}\right)-\nu^2F_0^2,$$

$$a_{21} = -a_{12}, \quad a_{22} = a_{11},$$

$$b_1 = k\frac{m_2}{d_0}+\frac{\nu^2}{k}\frac{L_0}{Ud_0}\left(1+\frac{m_1U}{\tau_0}\right)-\frac{\nu^2}{k}\frac{m_2}{d_0},$$

$$b_2 = k^2F_0^2\frac{m_2}{d_0}+\nu^2\frac{L_0}{Ud_0}F_0^2.$$

Then
$$c_r = \frac{a_{11}b_1 - a_{12}b_2}{a_{11}^2 + a_{12}^2}, \tag{27}$$

$$c_i = \frac{a_{11}b_2 + a_{12}b_1}{a_{11}^2 + a_{12}^2}. \tag{28}$$

6. Discussion of theory

c_r and c_i are both functions of the following six variables.

(i) Channel properties: (*a*) F_0, Froude number of the undisturbed flow; (*b*) $m_1 U/\tau_0$, dimensionless local slope of the resistance curve; (*c*) m_2/d_0, dimensionless local slope of the bed load transport curve; (*d*) L_0/Ud_0, concentration of bed load in the undisturbed flow.

(ii) Disturbance properties: (*a*) k, dimensionless wave-number; (*b*) $(n\pi/S_0)\,d_0/2b$, number of lanes into which the channel is divided longitudinally by the disturbance. Channel properties are also included, mean slope and aspect ratio of the cross-section.

If the properties of a particular flow in a particular channel are known, it is possible to calculate c_r and c_i for ranges of values of the disturbance properties. The sign of c_i identifies stable and unstable conditions and Uc_r is the speed of migration of the disturbance.

The value of n to be used for channels expected to meander is 1. Higher values of n subdivide the channel longitudinally and are related to braiding. A significant value of the wave-number can be obtained by following Kennedy (1963) and finding the maximum value of kc_i.

Thus, if c_r, c_i and kc_i are all computed as functions of k for a given flow in a given channel, meandering ($n = 1$) or braiding ($n > 1$) is predicted if $c_i > 0$ when kc_i is a maximum and the wavelength and speed of migration will be given by the corresponding values of k and c_r.

A general analysis of stability can be made. If $m_1 U/\tau_0 \neq 0$, a curve showing kc_i *versus* k passes through the origin with zero slope. When k is small,

$$kc_i \simeq \frac{\nu^2F_0^2 + \{1+(m_1U/\tau_0)\}^2}{\nu^2(m_1U/\tau_0)^2}\left[\frac{\nu^2F_0^2+\{1+(m_1U/\tau_0)\}}{\nu^2F_0^2+\{1+(m_1U/\tau_0)\}^2}\frac{m_2}{d_0} - \frac{L_0}{Ud_0}\right]k^2.$$

The rate of transport of bed load can be related to mean velocity by an empirical exponential relationship of the form $L_0 \propto U^N$, so that

$$m_2/d_0 = N(L_0/Ud_0).$$

Generally, ν is large and $m_1 U/\tau_0$ much smaller, and $N > 1$ so that the curve kc_i *versus* k turns upwards as sketched in figure 3. The curve passes through a maximum and approaches a horizontal asymptote. The maximum occurs with a positive value of c_i, so satisfying the condition for instability.

Stability would be possible only with $1+(m_1U/\tau_0)$ positive and m_1U/τ_0 big enough to make

$$\frac{\nu^2F_0^2+\{1+(m_1U/\tau_0)\}}{\nu^2F_0^2+\{1+(m_1U/\tau_0)\}^2}N < 1.$$

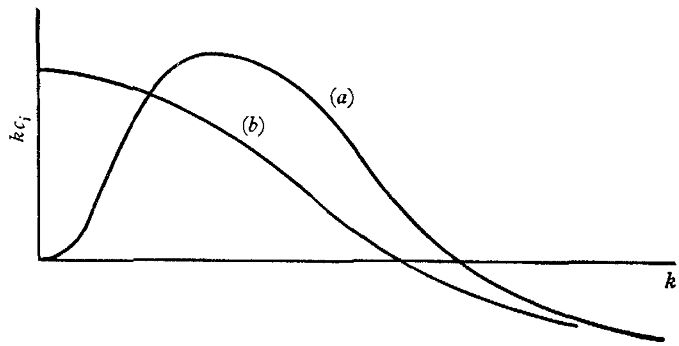

FIGURE 3. Sketches of kc_i *versus* k. Only the parts of the function for real positive values of k are shown. Curve (*a*) is for $m_1 U/\tau_0 \neq 0$ and curve (*b*) is for $m_1 U/\tau_0 = 0$. As $k \to \infty$ each curve tends to a horizontal asymptote given by

$$kc_i = -\frac{m_2/d_0}{(1-F_0^2)^2}\left(1+\frac{m_1 U}{\tau_0}\right).$$

This requires
$$\frac{m_1 U}{\tau_0} > (\tfrac{1}{2}N-1)+\sqrt{[(N-1)\,\nu^2 F_0^2+(\tfrac{1}{2}N)^2]},$$
which is much bigger than values expected to occur.

If $m_1 U/\tau_0 = 0$ the curve crosses $k = 0$ with zero slope and with

$$kc_i = \frac{\nu^2}{1+\nu^2 F_0^2}\left(\frac{m_2}{d_0}-\frac{L_0}{Ud_0}\right).$$

For small values of k
$$kc_i = \frac{pk^2+q}{rk^2+s},$$
where
$$p = -\left\{(1+\nu^2 F_0^2)\frac{m_2}{d_0}+\nu^2 F_0^4\frac{L_0}{Ud_0}\right\},$$
$$q = \nu^2(1+\nu^2 F_0^2)\left(\frac{m_2}{d_0}-\frac{L_0}{Ud_0}\right),$$
$$r = (1-F_0^2)^2+F_0^4+2\nu^2 F_0^4(1-F_0^2),$$
$$s = (1+\nu^2 F_0^2)^2.$$

Since $N > 1$, $kc_i > 0$ when $k = 0$. As far as the author knows, the combination $m_1 = 0$ with $F_0 > 1$ has not been observed, so that the curve showing kc_i *versus* k has a maximum at $k = 0$ and turns down to an asymptote as sketched in figure 3. However, if conditions can be such as to make the curve turn up, it must pass through a maximum with $c_i > 0$ to reach the asymptote. In neither case can the channel be stable.

Hence all feasible channels are unstable, large values of $m_1 U/\tau_0$ being excluded as impracticable.

Experiments described below provided data for numerical calculations, the work being done on an IBM 1130 computer.

7. Experiments

Three sets of experiments have been used to test the analysis. One comprises seven runs carried out in Auckland. The other two sets were selected from those described by Leopold & Wolman (1957). Five channels, in fine sand, were single thread channels and four in medium sand became braided.

The Auckland experiments were made in a tilting flume with a working section 40 ft. long by 8 ft. wide. It contains sand (mean size 0·45 mm) to a depth of 9 in. and is equipped with a sand feed by means of which dry sand can be fed into the experimental channel at a controlled rate. There is a balance at the downstream end so that the sand output rate can be measured. Water is circulated by means of a pump and the rate of flow is measured with an orifice meter or a bend meter. A detailed description of the apparatus has been published (Callander 1966).

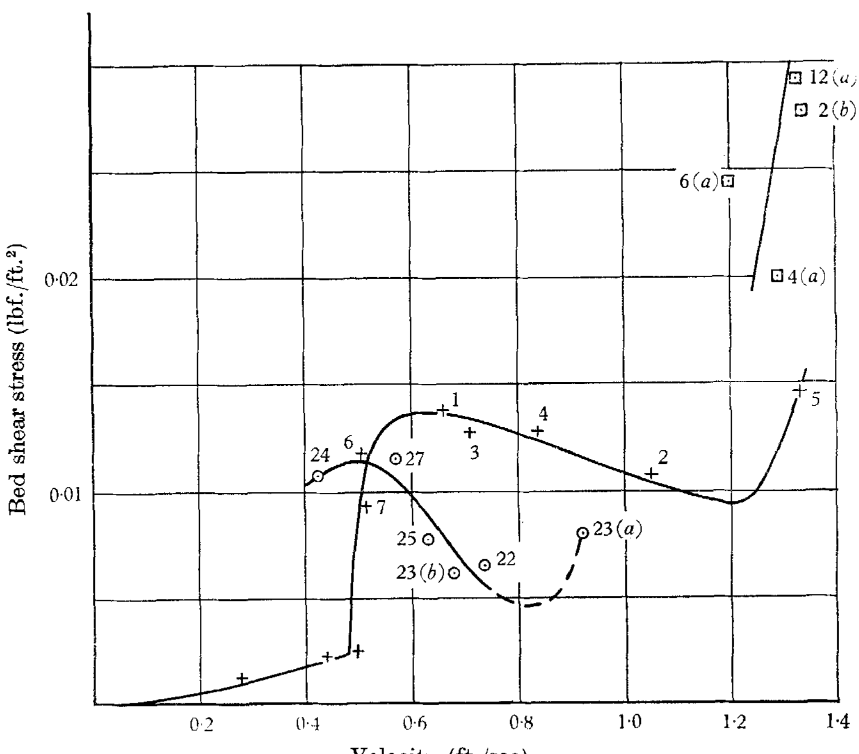

FIGURE 4. Bed shear stress *versus* mean velocity. Results identified by run number except for three flat bed runs at low velocity by Callander. +, Callander; ⊙, Leopold & Wolman, find sand; ⊡, Leopold & Wolman, medium sand.

For the stability tests a straight pilot channel with a trapezoidal section 5 in. deep, 10 in. wide at the bottom and 30 in. wide at the top was cut in the sand. Water was circulated at a constant rate for each run and sand was fed in at a constant rate. The rate of sand feed and the slope of the flume were chosen by trial and error so as to give approximately uniform flow in the fully developed channel. During development of a channel, its width increased, its depth decreased and a set of bed features was formed. The duration of individual runs ranged from 16 h to 2250 h.

When a channel was considered to be fully developed, measurements of water surface slope and cross-sections were made. From these, the mean bed shear stress, mean velocity, Froude number and rate of transport of bed load per unit width of channel were calculated.

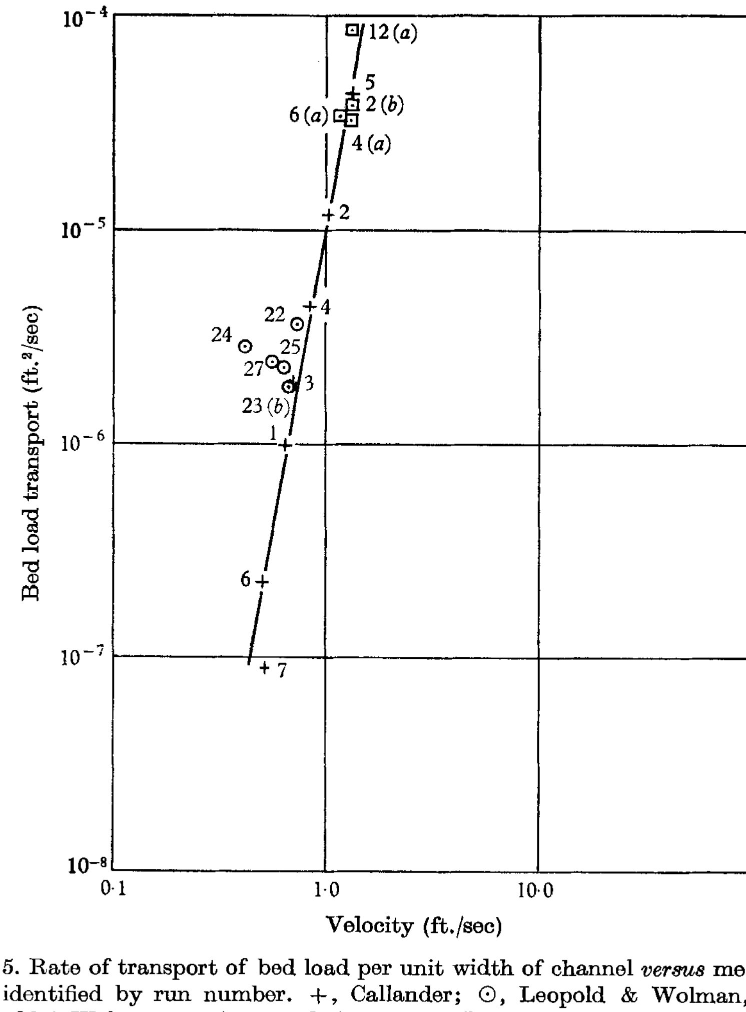

FIGURE 5. Rate of transport of bed load per unit width of channel *versus* mean velocity. Results identified by run number. +, Callander; ⊙, Leopold & Wolman, fine sand; ⊡, Leopold & Wolman, medium sand. Assumed bulk density 100 lb./ft.³.

The results of these measurements are shown on figures 4 and 5. In addition to data from runs 1–7, figure 4 shows three observations made on the pilot channel without bed features. One of these was just beyond the threshold of grain movement, the measurements being made before bed features had developed. The other two were at subthreshold velocities. On figure 5 the bed load transport and velocity are plotted on logarithmic scales and a least squares straight line has been drawn through the seven points. Its equation is

$$\frac{L_0}{1\cdot85\times10^{-6}} = \left\{\frac{U}{0\cdot755}\right\}^{5\cdot94}. \tag{29}$$

From these curves, the parameters $m_1 U/\tau_0$ and m_2/d_0 can be calculated for each run. The value of m_2/d_0 is most readily found from the concentration of bed load L_0/Ud_0 since the exponential relationship

$$L_0 \propto U^{5\cdot94} \tag{30}$$

leads to

$$\frac{m_2}{d_0} = 5\cdot94\frac{L_0}{Ud_0}.$$

Figure 4 gives the slope m_1 near each point and this has been used with the plotted values of U and τ_0 to give $m_1 U/\tau_0$.

The data from Leopold & Wolman are also plotted on figures 4 and 5. Using figure 4, $m_1 U/\tau_0$ was calculated as above and for m_2/d_0, equation (30) has been assumed to be valid.

The details of the results of the Auckland experiments are in table 1. Similar information is given by Leopold & Wolman for their channels.

Run no.	5	2	4	3	1	6	7
Discharge, ft.^{3}/sec	1·38	0·87	0·75	0·63	0·52	0·30	0·28
Bed load, lb./sec	327×10^{-4}	63×10^{-4}	29×10^{-4}	12×10^{-4}	5×10^{-4}	1×10^{-4}	$0\cdot35\times10^{-4}$
Bed load/ft., ft.^{3}/sec	433×10^{-7}	115×10^{-7}	$42\cdot0\times10^{-7}$	$19\cdot3\times10^{-7}$	$9\cdot7\times10^{-7}$	$2\cdot2\times10^{-7}$	$0\cdot88\times10^{-7}$
Slope	$1\cdot71\times10^{-3}$	$1\cdot23\times10^{-3}$	$1\cdot58\times10^{-3}$	$1\cdot43\times10^{-3}$	$1\cdot44\times10^{-3}$	$1\cdot42\times10^{-3}$	$1\cdot079\times10^{-3}$
Area, ft.^{2}	1·035	0·832	0·897	0·891	0·786	0·609	0·547
Breadth, ft.	7·56	5·99	6·90	6·23	5·15	4·58	3·96
Mean depth, ft.	0·137	0·139	0·130	0·143	0·153	0·133	0·139
Velocity, ft./sec	1·33	1·05	0·836	0·707	0·660	0·505	0·512
Bed shear, lbf./ft.^{2}	0·0146	0·0107	0·0128	0·0128	0·0137	0·0118	0·00935
Duration, hours	16	64	180	196	144	1097	2250
Classification	Unstable	Stable	Stable	Unstable	Unstable	Unstable	Unstable

TABLE 1

Table 2 contains the data used as input for the calculations for c_r, c_i and kc_i as functions of k and ν. For all channels except those in set 3, $n = 1$, being the value related to meandering. Leopold & Wolman reported the channels in set 3 as braided and figure 34 of their paper suggests that $n = 3$ and that the wavelength of the disturbance is of the same order of size as the width of the channel.

Values of c_r, c_i and k at the maximum of kc_i are given in table 3, where corresponding calculated wavelengths are also shown.

8. Discussion of results

The calculated values of c_i are all positive. It is not easy to test this conclusion because of the difficulty of defining an objective criterion for stability in the experimental channels. In runs 1, 3, 5, 6, 7, of set 1, an alternating pool and bar configuration could be seen on the bed at the end of the run and it was easy to

Run no.	$\frac{m_1 U}{\tau_0}$	$\frac{m_2}{d_0} = 5{\cdot}94 \frac{L_0}{Ud_0}$	$\frac{L_0}{Ud_0}$	F_0	$\frac{n\pi}{S_0}\frac{d_0}{2b}$	n
			Set 1. Callander			
1	−0·140	$57{\cdot}0 \times 10^{-6}$	$9{\cdot}60 \times 10^{-6}$	0·298	64·8	1
2	−0·869	468×10^{-6}	$78{\cdot}8 \times 10^{-6}$	0·496	59·4	1
3	−0·344	113×10^{-6}	$19{\cdot}1 \times 10^{-6}$	0·329	50·5	1
4	−0·597	229×10^{-6}	$38{\cdot}6 \times 10^{-6}$	0·408	37·5	1
5	+5·25	1412×10^{-6}	238×10^{-6}	0·633	33·3	1
6	+2·81	$19{\cdot}5 \times 10^{-6}$	$3{\cdot}28 \times 10^{-6}$	0·244	64·3	1
7	+8·98	$7{\cdot}36 \times 10^{-6}$	$1{\cdot}24 \times 10^{-6}$	0·242	102·3	1
			Set 2. Leopold & Wolman, fine sand			
22	−4·04	$6{\cdot}45 \times 10^{-4}$	$10{\cdot}88 \times 10^{-5}$	0·607	150	1
23(*b*)	−3·26	$21{\cdot}7 \times 10^{-4}$	$36{\cdot}6 \times 10^{-5}$	0·442	200	1
24	+0·785	$5{\cdot}95 \times 10^{-4}$	$10{\cdot}02 \times 10^{-5}$	0·290	100·5	1
25	−2·64	$4{\cdot}35 \times 10^{-4}$	$7{\cdot}33 \times 10^{-5}$	0·502	48·9	1
27	−1·203	$3{\cdot}34 \times 10^{-4}$	$5{\cdot}63 \times 10^{-5}$	0·368	61·8	1
			Set 3. Leopold & Wolman, medium sand			
2(*b*)	+6·93	$3{\cdot}22 \times 10^{-3}$	$5{\cdot}43 \times 10^{-4}$	1·025	44·3	3
4(*a*)	+9·15	$3{\cdot}03 \times 10^{-3}$	$5{\cdot}10 \times 10^{-4}$	1·017	45·0	3
6(*a*)	+7·00	$3{\cdot}08 \times 10^{-3}$	$5{\cdot}19 \times 10^{-4}$	0·900	50·2	3
12(*a*)	+6·50	$6{\cdot}91 \times 10^{-3}$	$11{\cdot}67 \times 10^{-4}$	0·998	42·9	3

TABLE 2

Run no.	c_r	c_i	k	λ ft.	Width ft.
		Set 1. Callander			
1	$2{\cdot}322 \times 10^{-5}$	$5{\cdot}932 \times 10^{-5}$	8·5	78·5	—
2	$1{\cdot}289 \times 10^{-4}$	$1{\cdot}198 \times 10^{-4}$	11	64·5	—
3	$4{\cdot}298 \times 10^{-5}$	$7{\cdot}330 \times 10^{-5}$	10	62·8	—
4	$8{\cdot}339 \times 10^{-5}$	$9{\cdot}734 \times 10^{-5}$	9	57·5	—
5	$6{\cdot}785 \times 10^{-4}$	$1{\cdot}631 \times 10^{-4}$	24	21·0	—
6	$6{\cdot}691 \times 10^{-6}$	$9{\cdot}963 \times 10^{-7}$	29·5	20·0	—
7	$4{\cdot}520 \times 10^{-6}$	$1{\cdot}349 \times 10^{-6}$	130·5	6·20	—
		Set 2. Leopold & Wolman, fine sand			
22	$1{\cdot}42 \times 10^{-4}$	$4{\cdot}17 \times 10^{-5}$	25	6·52	—
23(*b*)	$5{\cdot}05 \times 10^{-4}$	$1{\cdot}802 \times 10^{-4}$	36	7·36	—
24	$8{\cdot}46 \times 10^{-5}$	$1{\cdot}67 \times 10^{-4}$	29	4·25	—
25	$1{\cdot}36 \times 10^{-4}$	$4{\cdot}89 \times 10^{-5}$	13·5	7·05	—
27	$1{\cdot}13 \times 10^{-4}$	$7{\cdot}81 \times 10^{-5}$	17	8·89	—
		Set 3. Leopold & Wolman, medium sand			
2(*b*)	$1{\cdot}55 \times 10^{-3}$	$1{\cdot}76 \times 10^{-4}$	25	1·40	1·19
4(*a*)	$1{\cdot}49 \times 10^{-3}$	$1{\cdot}95 \times 10^{-4}$	26	1·52	1·32
6(*a*)	$1{\cdot}47 \times 10^{-3}$	$1{\cdot}86 \times 10^{-4}$	30	1·43	1·28
12(*a*)	$3{\cdot}235 \times 10^{-3}$	$3{\cdot}953 \times 10^{-4}$	24	1·52	1·27

TABLE 3

classify these as unstable. The bed in runs 2 and 4 was classified as stable, but this may have been wrong. As shown in table 3, the calculated wavelength is longer than the flume for some runs, including these two.

Leopold & Wolman did not comment on the configuration of their channels in fine sand. However, they draw attention to the rarity of straight channels and it is assumed that their experimental channels in fine sand formed meanders, or would have formed meanders had the experiments continued.

The channels of Leopold & Wolman which became braided (set 3) can be classified as unstable.

Numerical calculations classified all sixteen channels as unstable, consistent with the general analysis. In nine cases, the appearance of the channel confirmed the instability. In the other seven, the disagreement was not conclusive.

The wavelengths have been calculated using Kennedy's criterion. Provided $m_1 U/\tau_0 \neq 0$, no difficulty arises from use of this criterion, but if $m_1 U/\tau_0 = 0$, it gives $k = 0$ and the only solution for (16)–(19) is the trivial one

$$A = B = D = H = 0.$$

However, k need be only infinitesimally greater than zero to permit non-zero values for A, B, D and H with the same value of kc_i. Alternatively, a small departure from zero in $m_1 U/\tau_0$ would allow the criterion to give a realistic solution; and such a departure is plausible if some uncertainty is allowed in assigning a value to $m_1 U/\tau_0$. These considerations lead to the conclusion that another criterion for instability might be more useful. It is suggested that instability will occur for k between those values which make kc_i greater than 0·95 (or a similar arbitrary fraction) of its maximum. The perturbation with the largest early amplitude is one of this set. Its wavelength is not known, but is assumed to be within the range given by the above criterion.

Table 4 shows the range of wavelengths estimated in this way for the channels in sets 1 and 2. Also shown is the range for data interpolated from set 1 with $m_1 = 0$.

For each channel, the predicted range of wavelength is compared with the empirical rule given by Inglis (1949)

$$M_L = 36Q^{0\cdot 5}.$$

The predicted wavelengths are all compatible with Inglis's observations.

In the case of the braided channels, the wavelengths have been calculated using the Kennedy criterion (table 3) and the modified criterion (table 4). They are of the same order of size as the widths of the channels, and this is reasonable.

9. Conclusions

The linearized stability analysis using a simplified description of the flow shows that channels with loose boundaries are unstable, with the possible exception of channels just beyond the threshold of grain movement. This exception is not important in practice because such conditions are unlikely to occur. Realistic estimates of the wavelengths in meandering and braided channels can also be made.

Run no.	$36Q^{0.5}$	Width	k	Wavelength
		Set 1. Callander		
1	26·0	—	4·7–15·0	47–149
2	33·6	—	7·6–15·8	45–93
3	28·6	—	6·9–14·6	43–92
4	31·2	—	6·6–12·0	43–78
5	42·4	—	20·7–28·2	18–24
6	19·7	—	19·5–38·3	15–30
7	19·0	—	113–151	5·4–7·2
		Interpolated ($m_1 = 0$)		
	25·0	—	0–110	> 60·1
		Set 2. Leopold & Wolman, fine sand		
22	4·84	—	18·5–32·0	5·1–8·8
23(*b*)	6·55	—	27·2–46·9	5·7–9·7
24	4·70	—	20·0–42·7	2·9–6·2
25	6·25	—	11·0–16·0	6·0–8·6
27	8·23	—	12·9–21·0	7·2–11·7
		Set 3. Leopold & Wolman, medium sand		
2(*b*)	—	1·19	20·5–27·5	1·27–1·71
4(*a*)	—	1·32	22·4–29·2	1·35–1·76
6(*a*)	—	1·28	25·0–34·2	1·26–1·72
12(*a*)	—	1·27	19·8–27·0	1·35–1·84

TABLE 4

No other conclusions can be drawn from the analysis about the flow as the amplitude of the disturbance grows because important characteristics of curved flows are omitted. In particular, secondary currents affect the distribution of fluid momentum and bed material, if the curvature is not very small.

I am grateful to Professors N. A. Mowbray, C. M. Segedin and A. J. Raudkivi for their help and advice during the progress of this research.

Equipment used in the Auckland experiments was purchased with grants from the New Zealand Universities' Research Grants Committee.

REFERENCES

CALLANDER, R. A. 1966 Construction of an experimental meander. *Proc. 2nd Australasian Conference on Hydraulics and Fluid Mechanics*. University of Auckland.

HANSEN, E. 1967 The formation of meanders as a stability problem. *Copehnagen Technical University of Denmark*. Basic Research Report no. 13.

INGLIS, C. C. 1949 The behaviour and control of rivers and canals. *Central Waterpower, Irrigation and Navigation Research Station. Poona.*

KENNEDY, J. F. 1963 The mechanics of dunes and antidunes in erodible bed channels. *J. Fluid Mech.* **16**, 521–544.

KENNEDY, J. F. & BROOKS, N. H. 1965 Laboratory study of an alluvial stream at constant discharge. *California Institute of Technology, Pasadena.* Report no. KH-R-17.

LEOPOLD, L. B. & WOLMAN, M. G. 1957 River channel patterns: braided, meandering and straight. *Geological Survey Professional Paper* 282-B. U.S. Government Printing Office, Washington.

Raudkivi, A. J. 1963 Study of sediment ripple formation. *Proc. Am. Soc. Civ. Engs* **89**. no. HY 6, 15–33.

Raudkivi, A. J. 1967 An analysis of resistance in fluvial channels. *Proc. Am. Soc. Civ. Engs* **93**, no. HY 5, 73–84.

Reynolds, A. J. 1965 Waves on the erodible bed of an open channel. *J. Fluid Mech.* **22**, 113–133.

Vanoni, V. A. & Brooks, N. H. 1957 Laboratory study of the roughness and suspended load of alluvial streams. *California Institute of Technology, Pasadena.* Report no. E-68.

White, C. M. 1939 The influence of transported solids upon rivers. Unpublished proof received privately from J. R. D. Francis.

White, C. M. 1948 Extrait des procès verbaux des séance de l'Assemblée d'Oslo (19–28 août 1948) de l'Union Geodesique et Geophysique Internationale. *British National Committee for Geodesy and Geophysics.*